

Modelling of the Hungarian spread of COVID-19 and control strategies with risk-based approach

Zsuzsa Farkas (✉ Farkas.Zsuzsa@univet.hu)

University of Veterinary Medicine

Tekla Engelhardt

University of Veterinary Medicine

Erika Ország

University of Veterinary Medicine

Miklós Süth

University of Veterinary Medicine

Szilveszter Csorba

University of Veterinary Medicine

Ákos Józwiak

University of Veterinary Medicine

Research Article

Keywords: COVID-19, epidemiological modelling, control strategies, risk-based testing, super-spreader identification, network analysis

Posted Date: December 15th, 2020

DOI: <https://doi.org/10.21203/rs.3.rs-117430/v1>

License:  This work is licensed under a Creative Commons Attribution 4.0 International License.

[Read Full License](#)

11 **Abstract**

12 **Background**

13 Novel Coronavirus Disease (COVID-19), caused by Severe Acute Respiratory Syndrome
14 Coronavirus 2 (SARS-CoV-2), threatens humanity in terms of health and economy as it spreads
15 extremely fast and causes massive epidemics all over the world. In the absence of a vaccine, social
16 isolation and hygienic measures are the only way to curb the virus.

17
18 **Methods**

19 In our study, the Hungarian spread of COVID-19 is modelled by applying a modified SEIR
20 (Susceptible, Exposed, Infected, Recovered) compartment model, which takes into account the route
21 of disease transmission not only from infected, but from latent individuals (exposed compartment) as
22 well. The differences between the modified model and the traditional SEIR model has been
23 evaluated. The different scenarios of disease spreading simulate the effect of the different level of
24 interventions (social distancing and hygienic measures) taken place in Hungary. The modelling also
25 considers the population and mobility data which are also essential in case of infectious disease
26 spreading. For controlling the disease in the long-term a network-based analysis is provided based on
27 the concept of the epidemic threshold and the identification of super-spreader population groups.

28
29 **Results**

30 According to sensitivity analysis of the modified SEIR model, disease transmission of latent
31 individuals has the greatest effect on the number of infections. Based on the results, the applied
32 interventions have a great impact on the disease spreading and are effective in controlling the
33 COVID-19 epidemic., a network-based analysis is provided based on the concept of the epidemic
34 threshold and the identification of super-spreader population groups. According to the results of the
35 network-based study, the proportion of people to be sampled for an effective disease control is the
36 function of the identified people with high number of contacts in social networks who act as super-
37 spreaders.

38
39 **Conclusion**

40 Applying network-based random, selective and targeted sampling, testing and isolation of affected
41 individuals would yield significantly different sample sizes, highlighting the importance of super-
42 spreaders. Network analysis (but also all computational science methods) need large amount of good
43 quality data and the spread of these methods could be supported by easy-to-use tools. We wanted to
44 raise awareness also on this issue.

45 **Keywords:** COVID-19, epidemiological modelling, control strategies, risk-based testing, super-
46 spreader identification, network analysis.

47 **Background**

48 Genetic mutations of microorganisms are inevitable, however, due to climate crisis and other crucial
49 drivers of change, emerging infectious diseases are more and more likely to threaten humanity in the
50 near future. Nowadays, mankind is in a great crisis in terms of health and economy because of an
51 epidemic caused by the mutation of an originally animal-related coronavirus (1)(2). By adapting to
52 humans, the virus named Severe Acute Respiratory Syndrome Coronavirus 2 (SARS-CoV-2) (3)
53 caused pandemic infectious disease COVID-19 (4) that affects millions of lives. As of today, it has
54 appeared almost all over the world, it spreads extremely fast and causes massive epidemics.

55 COVID-19 is transmitted by inhalation or contact with infected droplets (5,6). It must be noted that
56 the aerosol and surface stability of SARS-CoV-2 is higher than SARS-CoV-1, therefore indirect
57 transmission routes are more significant than previously thought (7,8).

58 In the absence of a vaccine, social isolation and hygienic measures are the only way to curb the virus.
59 However, these interventions are proved to be effective only when applied very strictly because of
60 the very high virulence of SARS-CoV-2 (9,10). The level of isolation needed (e.g. school closures,
61 banned events and gatherings) is such high that it is unsustainable in the long run.

62 Modelling is a key option in epidemiology in cases when limited data are available regarding an
63 infectious disease like emerging diseases such as COVID-19. Scenario analysis is a tool by which
64 information can be gained that can support decision making regarding mitigation strategies and risk
65 management, nevertheless, it has its limitations which must be taken into account. As of today,
66 several publications have already appeared which have attempted to simulate the spread of COVID-
67 19 from different aspects. Most of the earliest publications study the epidemic in China by applying
68 the SEIR (Susceptible, Exposed, Infected, Recovered) compartment model with different
69 modifications depending on the purpose of the modelling. Some publications try to estimate the
70 extent of the epidemic regarding time period and number of total infections (11,12), while most of
71 the studies model the effect of interventions such as isolation and quarantine (13–18).

72 As time goes by, more and more information is available regarding the disease dynamics and disease
73 characteristics of COVID-19, thereby epidemiological models and parameters of the models can
74 more precisely be determined. One of the most important finding is that there are many latent people
75 who develop no symptoms or only mild symptoms, and the disease is infectious in the latent phase as
76 well. Therefore, many people carry and transmit the virus, thereby contribute to the spread of the
77 disease in an unnoticeable way (19–23). Most of the earlier research did not account for this type of
78 transmission because of the lack of knowledge, though it would be essential in understanding the
79 disease dynamics (24).

80 Conventional compartment models try to capture state transitions and simulate the course of disease
81 in a uniform and homogenous population. However, the basic assumption that any person can contact
82 anyone, and everyone has the same number of contacts, is not true in the real social networks.

83 Many real networks share same characteristics and are surprisingly similar to each other. These
84 networks are sparse, where many nodes with small number of contacts are connected with each other
85 through few large hubs with many contacts. The number of contacts a node has is denoted by k , and
86 is called the degree of the node. If the degree distribution of a network follows a power law, it is
87 called a *scale-free network* (25). In scale-free networks, compared to random networks, nodes can
88 have very different degrees, ranging from very small, to huge (which are called hubs). Thus, the
89 average degree is not enough in itself to describe the network topology. Diseases can spread much

90 faster in such networks due to the presence of super-spreader hubs. These networks are also known
91 for their specific robustness: they withstand untargeted attacks without falling apart, but they are
92 vulnerable to attacks targeting the large hubs of the network. This phenomenon could also be used
93 for planning targeted interventions.

94 The aim of this study is to present an epidemiological modelling based on the SEIR compartment
95 model that is generally accepted for modelling the spread of COVID-19, but with a modification in
96 order to take the transmission route of the latent, yet infectious people into account. Network
97 analysis-based intervention strategies are also discussed in the paper, since the profound implications
98 of network theory are not widely known in the public health community.

99

100 **Materials and Methods**

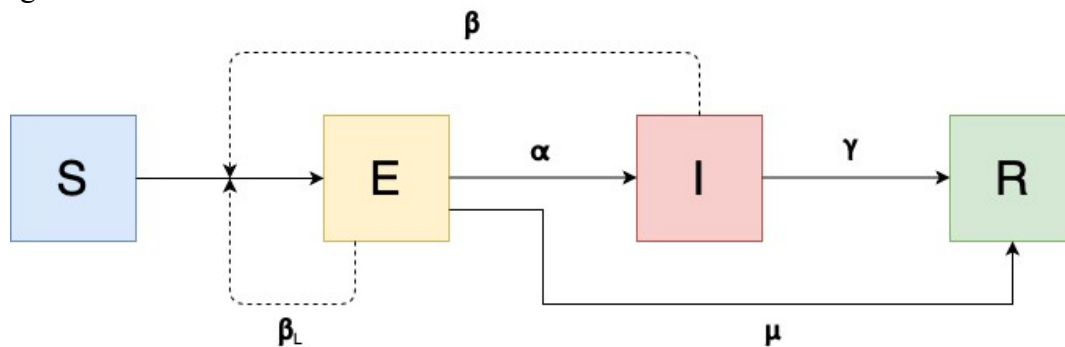
101 **Structure of the epidemiological model**

102 **Modified SEIR model for COVID-19**

103 For COVID-19, we have built a SEIR (Susceptible, Exposed, Infected, Recovered) compartment
104 model for a basis of the modelling but we have applied some modifications. In the original SEIR
105 model, the Exposed compartment is not infectious. Our modified SEIR model accounts for the
106 infectiousness of this compartment ‘E’, as it has been shown by previous studies (19–23), and also
107 account for a route of transition of being recovered without symptoms or with mild symptoms from
108 the Exposed compartment to the Recovered compartment. For better differentiation from the original,
109 SEIR model with the applied modifications will be referred as ‘modified SEIR model’ (Figure 1.),
110 and individuals in Exposed compartment are called ‘latent’.

111

112 **Figure 1**



113 Structure of the modified SEIR model with compartment initials (Susceptible, Exposed (Latent),
114 Infected, Recovered), transitions from one compartment to another (full line), parameters and routes of
115 infection (dashed line). Susceptible individuals can get the infection either from individuals being in the
116 Infected compartment with the rate of β , or from Exposed compartment (latent individuals) with the rate
117 of β_L .

118

119 The following differential equations describe the dynamics of the modified SEIR model (1):

$$\begin{aligned}
120 \quad & \frac{dS}{dt} = -\beta_L SE - \beta SI, \\
121 \quad & \frac{dE}{dt} = \beta_L SE + \beta SI - \alpha E - \mu E, \\
122 \quad & \frac{dI}{dt} = \alpha E - \gamma I \\
123 \quad & \frac{dR}{dt} = \gamma I + \mu E \tag{1}
\end{aligned}$$

124 where S, E, I and R are the fractions of Susceptible, Exposed, Infected and Recovered individuals,
125 and S+E+I+R=1 at all times.

126 Parameters of the model

127 Selection of values for different model parameters has been done by literature research. There were
128 many estimations in previous publications for the value of basic reproduction number, R_0 , ranging
129 from 1.95 (1.4-2.5) (26) to 6.47 (95% CI 5.71–7.23) (27). Our model has been built to be consistent
130 with the average range of reported R_0 values. The mean value of the incubation period was
131 consistently around 4 to 6 days in numerous publications (12,28–31), therefore we selected the
132 number of latent days to be 5 (transition rate from Exposed compartment to Infected compartment).
133 3.5 days of infectious period was chosen for the calculation of recovery rate, following the studies of
134 Li et al. (19) and Tang et al. (27). The transition rate from Exposed compartment to Recovered
135 compartment arises from the number of days latent individuals spend while carrying and transmitting
136 the virus, which in our model is the sum of incubation period and infectious period, therefor 8.5 days.

137 The parameter values in the baseline scenario (*Scenario 1*) with no interventions are shown in Table
138 1.

139 Table 1. Definitions and values of the modified SEIR model parameters

	Definition	Number of days	Value (day ⁻¹)
α	Transition rate from Exposed compartment to Infected compartment	5	0.2
γ	Recovery rate	3.5	0.29
μ	Transition rate from Exposed compartment to Recovered compartment	8.5	0.12
β	Transmission rate		0.8*
β_L	Latent transmission rate		0.4*

140 *Approximate values considered to be in line with the average reported R_0 values (32,33). These parameters will change
141 in Scenarios 2 and 3.

142
143 According to Wu et al. (18) and Nishiura et al. (21), latent individuals are able to transmit the
144 infection 50% less than infected individuals. This is in line with other studies regarding

145 asymptomatic transmission rate of 50% in case of influenza (34,35). Therefore, the rate β_L (beta
146 latent) will be half of the β value.

147

148 **Limitations of the compartment model**

149 The formulation was made assuming that natural birth rate is equal to natural mortality rate, therefore
150 the observed dynamics are considered to be caused by the disease. Individual differences, that could
151 influence the susceptibility of people such as age, gender, general health condition cannot be taken
152 into account, all individuals are considered equally susceptible for the disease.

153 **GLEAMviz software**

154 Simulations were performed with the publicly available GLEAMviz Simulation System (36), that is a
155 scientific application designed for performing simulations of the spread of infectious diseases. With
156 the real-world demographic and mobility data, location and time of potential virus transmission by
157 human interactions can be simulated. Compartment model in the Simulation System is customizable,
158 thereby can be adapted for various infectious diseases. The spread of the infection among individuals
159 is driven by the characteristics of the disease specified in the compartment model (37–39).

160 **Setting options regarding compartment models in GLEAMviz**

161 Number of compartments and transitions from one compartment to another (infectious or
162 spontaneous) can arbitrarily be defined. In case of each compartment, air travel and commuting can
163 be allowed or disallowed and there are 3 ways for the settings of infectiousness for each
164 compartment: 1. Carrier 2. Clinical 3. None.

165 **Other setting options in GLEAMviz**

166 Simulations can be done with single run or multiple runs, in latter case, the number of runs can be
167 defined, and the results can be retrieved with median and confidence interval values calculated over
168 the set of runs. Start date and duration of the simulation can be set. GLEAM uses robust statistical
169 methods and executes the simulation in a sequence of time steps that represents full days. Average
170 percentage of airline traffic can be set. For each simulated flight, the number of passengers is a
171 stochastic variable sampled from a binomial distribution whose mean is given by the airline traffic
172 value times the number of bookings. There is an option for enabling seasonality with a built-in
173 algorithm that rescales the basic reproduction ratio R_0 by a sinusoidal function. For commuting
174 model, one can choose from gravity (40) or radiation (41) models. Users can set the average number
175 of hours spent by the commuters at the commuting destination. The default value is 8 hours (the
176 average amount of working time in a day). Minimum number of clinical cases that need to occur in a
177 country for it to be considered infected and minimum number of infected countries for a global
178 epidemic to be considered to occur can be set. Initial population composition for each compartment
179 can be specified in percentages of the total global population. Initial epidemic locations (cities) and
180 number of individuals in the given compartment can be defined for arbitrary number of initial
181 epidemic seeds.

182 The so-called ‘exceptions’ panel in GLEAMviz provides a way to specify time and space dependent
183 changes of the variable values defined in the compartment model. Each exception lets the user define
184 alternative values for one or more variables for a specified period and specified areas (e.g. cities,
185 countries).

186

187 **Basic scenarios for modelling disease spread in Hungary with interventions**

188 **Scenario 1 – ‘worst case’**

189 Worst case scenario with no specific interventions, model parameters determined in the above section
190 ‘Parameters of the model’. It represents the conditions of the beginning of the epidemic in Hungary
191 (04 March 2020) (COVID-19 pandemic in Hungary, 2020). It is assumed that only infected
192 individuals with serious and founded COVID-19 symptoms are quarantined in Hungary.

193 Regarding interventions, our assumption is that all interventions applied (social isolation and
194 hygienic measures) overall decrease the rate of virus transmission, in our case β and β_L values which
195 is in line with the theory of Li et al. (19) and Ferguson et al. (15). Therefore, in case of scenarios with
196 interventions (Scenarios 2, 3), only these parameter values are decreased proportionally depending on
197 the extent of the effect of interventions.

198 **Scenario 2 – First round of interventions**

199 In Hungary, from 16 March 2020, schools and universities operate by distance-learning, nursery
200 schools and other pre-school establishments only provide duty service, more and more employers
201 provide the opportunity of home office for the workers and people are getting conscious about
202 staying at home and reducing the physical contacts as much as possible. Events with large number of
203 people were banned (the limit was 100 people for indoor and 500 for outdoor events, respectively).
204 According to our assumption that is supported by the data of Google Analytics (42) and Hungarian
205 traffic statistics (43), that means a 50% decrease in the level of social interactions compared to the
206 normal lifestyle. This, together with the raised awareness of the disease and the importance of
207 detection and quarantine of infected people, based on the approach of Ferguson et al. (15) results in
208 the decrease of β and β_L values to 0.4 and 0.2 (from 0.8 and 0.4), respectively.

209 **Scenario 3 – Second round of interventions**

210 From 28 March, the Hungarian government have ordered curfew restrictions across the country, in
211 the first round until the 11th of April, and in the second round it was extended for an indefinite period.
212 The goal of the restrictions was generally to limit the contact of people who do not live in the same
213 household, therefore residences should only be left for the satisfaction of basic needs (e.g. work,
214 grocery, pharmacy, health services) the previously specified restrictions regarding the institutions
215 have remained unchanged. According to our assumption and the further mentioned references (42,43)
216 that resulted in a further 25%, altogether 75% reduction in the level of social interactions compared
217 to the normal lifestyle, which means a reduction in β and β_L values to 0.3 and 0.1, respectively.

218 Scenarios 1 to 3 attempt to model the real-life situation regarding disease spreading with the
219 temporally applied intervention measures in Hungary. It is noted, however, that the list of
220 interventions is not fully complete, only those are mentioned which are crucial regarding scenario
221 building.

222 **Practical implementation in GLEAMviz (Settings)**

223 Unless not specifically indicated, settings are applied for each four Scenarios.

224 ‘MODEL’ panel: Modified SEIR model (Figure 1.) with parameters defined in section ‘Parameters of
 225 the model’. Special GLEAMviz setting options for different compartments are shown in Table 2.

226 Table 2. Special GLEAMviz setting options in different compartments

	Susceptible	Exposed (Latent)	Infected	Recovered
Infectiousness	none	carrier*	clinical**	none
Commuting	allowed	allowed	disallowed	allowed
Air travel	allowed	allowed	disallowed	allowed

227 *: *but transmitting the virus with the rate of β_L*

228 **: *transmitting the virus with the rate of β*

229

230 ‘SETTINGS’ panel:

- 231 ▪ Multi-run simulation (20 runs, the maximum possible number of runs)
- 232 ▪ Start date: 4 March 2020 - the date of the first reported cases of SARS-CoV-2 infection (44)
- 233 ▪ Airline traffic:
 - 234 • *Scenario 1*: 88% (12% decrease globally in the first half of March according to OAG
 - 235 statistics) (45)
 - 236 • *Scenario 2*: 52% (48% decrease globally in the second half of March) (45)
 - 237 • *Scenario 3*: 30% (66% decrease rounded up to 70% as data were available only until 20
 - 238 April 2020)(45)
- 239 ▪ Commuting model: radiation model was chosen as it is proved to describe the commuting
- 240 patterns better when parameter-free algorithms must be used (41,46).
- 241 ▪ Time spent at commuting destination:
 - 242 • *Scenario 1*: 8 hours (default, assuming no change at commuting in Hungarian region)
 - 243 • *Scenario 2*: 4 hours (50% reduction in commuting according to Hungarian traffic
 - 244 statistic)(42,43)
 - 245 • *Scenario 3*: time spent at commuting destination: 2 hours (75% reduction in commuting
 - 246 according to Hungarian traffic statistic) (42,43)
- 247 ▪ Seasonality: disabled – as it is believed that SARS-CoV-2 is not affected by weather parameters
- 248 and there is no evidence to the contrary at the moment (47).
- 249 ▪ Minimum number of clinical cases that need to occur in a country for it to be considered
- 250 infected: 1 (default)
- 251 ▪ Minimum number of infected countries for an occurrence to be an epidemic: 2 (default)
- 252 ▪ Initial global distribution of a population in compartments: 100% susceptible
- 253 ▪ Initial geographic location of the epidemic: Officially 2 infected people were registered on the
- 254 4th of March 2020 in Hungary (48), Budapest, but in order to get more realistic simulations
- 255 regarding the coverage of the region, initially 5 infected individuals were set for Budapest and
- 256 3, 3 latent individuals for Debrecen and lake Balaton, based on population data, respectively.
- 257 These were the only available locations in GLEAMviz software for Hungary.
- 258 As there is a possibility for setting numerous initial locations of the epidemic, number of
- 259 individuals with registered COVID-19 infections (number of active patients) were collected for
- 260 the 4th of March, 2020. Only cities can be set in the software, and data about registered

261 infections were available in different levels of aggregation. Table 3. shows the initial locations
 262 with number of infected people used in the simulation (only >20) apart from Hungary.
 263

264 Table 3. Initial locations and number of infected individuals (apart from Hungary) set in GLEAMviz.

Initial location		No. of infected individuals	Level of aggregation of the data	Reference
Country	City			
Austria	Innsbruck	22	national (halved)	(49)
	Vienna	21	national (halved)	
France	Lille	65	regional	(50)
	Lyon	49	regional	
	Strasbourg	38	regional	
	Paris	55	regional	
Germany	Düsseldorf	115	federal state	(51)
	Munich	48	federal state	
	Stuttgart	50	federal state	
Italy	Ancona	80	regional	(52)
	Bologna	516	regional	
	Florence	37	regional	
	Milan	1497	regional	
	Naples	31	regional	
	Rome	27	regional	
	Turin	82	regional	
	Venice	345	regional	
Spain	Barcelona	24	autonomous community	(53)
	Madrid	90	autonomous community	
China	Beijing	1267	national except Hubei	(54)
	Wuhan	24085	Hubei province	
Iran	Tehran	2259	national	(54)
Japan	Tokyo	278	national	(55)
Singapore	Singapore	33	national	(56)
South Korea	Seoul	5547	national	(57)

265

266 Settings of ‘EXCEPTIONS’ panel are shown in Table 4.

267 Table 4. ‘EXCEPTIONS’ panel settings in GLEAMviz.

No. of Scenario	Exception(s) applied	
<i>Scenario 1</i>	No exceptions applied	
<i>Scenario 2</i>	$\beta = 0.4$; $\beta_L = 0.2$; from 16 March 2020 till the end of the simulation; in the Hungarian region	
<i>Scenario 3</i>	$\beta = 0.4$; $\beta_L = 0.2$; from 16 March 2020 to 27 March 2020; in the Hungarian region	$\beta = 0.3$; $\beta_L = 0.1$; from 28 March 2020 till the end of the simulation; in the Hungarian region

268

269 Comparison of modified SEIR model with traditional SEIR model

270 In order to evaluate the differences between modified SEIR model and the traditional (‘basic’) SEIR
271 model, a simulation has been made in which parameters β_L and μ were disregarded (transition rates
272 that contribute to the infectiousness of exposed individuals). Other parameters and settings were the
273 same as in Scenario 1 in the simulation.

274 Sensitivity analysis of modified SEIR model

275 The sensitivity analysis has been done to reveal the parameter(s) to which the model is the most
276 sensitive. There were five parameters in our modified SEIR model to be investigated: β , β_L , γ , α , μ .
277 The parameters and settings of *Scenario 1* was used for the evaluation. The maximum value of the
278 daily number of individuals in the infected compartment and the number of days related to this value
279 were selected as the endpoint. Only one parameter per scenario was changed at a time. Changes in
280 both directions were evaluated with lower ($\times \frac{1}{2}$) and higher ($\times 2$) values compared to the baseline
281 value (Table 1.) of the examined parameter.

282 Network analysis-based intervention strategies

283 The basic assumption of the conventional compartment models is that any person can contact
284 anyone, and everyone has the same number of contacts, is not true in the real contact networks. Real
285 networks are sparse, where many nodes with small number of contacts are connected with each other
286 through few large hubs with many contacts, which could also be identified as super-spreaders.

287 The first applications of network science to disease modelling set a new scientific field called
288 network epidemics (58). When modelling disease spreading, the network characteristics will yield
289 many important differences compared to the conventional compartment models.

290 First of all, the diseases spread much faster in scale free networks due to the presence of hubs. In
291 network epidemics the concept of *epidemic threshold* (λ_c) is used: pathogens can only spread if the
292 spreading rate λ exceeds λ_c . The spreading rate can be defined as:

293
$$\lambda = \frac{\beta^*}{\mu} \quad (2)$$

294 where β^* is the likelihood that the disease will be transmitted from one infected person to a
295 susceptible one in a unit of time, and μ is the recovery rate. The conventional R_0 can be defined as:

$$296 \quad R_0 = \langle k \rangle \lambda \quad (3)$$

297 where $\langle k \rangle$ is the average degree. In case of scale free networks, the epidemic threshold is:

$$298 \quad \lambda_c = \frac{1}{\frac{\langle k^2 \rangle}{\langle k \rangle} - 1} \quad (4)$$

299 where $\langle k^2 \rangle$ is the second moment of the degree distribution, and it is used in the calculation of the
300 variance (25). In scale free networks, $\langle k^2 \rangle$ is significantly larger than $\langle k \rangle$, due to the huge variance in
301 degrees of the nodes. This means, that in large scale-free networks λ_c is very small, meaning that
302 most of the diseases can spread very rapidly because of the presence of large hubs. This holds for
303 every network (not only scale-free ones), where there is a large difference between the degrees of the
304 nodes. This phenomenon was also captured by Meyers et al. (59), who applied the methods of
305 contact network epidemiology for SARS, to illustrate that for a single value of R_0 , any two outbreaks,
306 even in the same setting, may have very different epidemiological outcomes.

307 Many social contact networks are also scale-free networks. We don't have a map of the Hungarian
308 contact network of people, but we can estimate λ_c with the use of other data. The Copenhagen
309 Networks Study resulted in a multi-layer temporal network which connects a population of more than
310 700 university students over a period of four weeks (60). We have used a 2-week (common agreed
311 suggested quarantine period)(61) subset of the network of physical proximity among the participants
312 (estimated via Bluetooth signal strength) to simulate direct personal contacts. We have used the
313 settings defined by Stopczynski et al. (62): only contacts where the signal strength was ≥ -75 dBm
314 were used, corresponding to distances of approximately 1 meter or less. Based on these data, a
315 network had been constructed and analysed with the use of KNIME free and open-source data
316 analytics (63), reporting and integration platform and igraph R-package (64).

317 Other important consequence of network topology is the difference in planning intervention
318 strategies. If we try to remove nodes from the network either with immunization (which we can't
319 perform yet in case of COVID-19) or with identifying latent and infected people with sampling and
320 testing, and then removing them with quarantine measures, we may have use other than conventional
321 options as well. For assessing the effect of identifying and removing latent and infected people with
322 sampling, testing and consequent quarantine measures, we use the concept of critical immunization
323 well established in network epidemiology. Critical immunization g_c is the proportion of nodes needed
324 to be removed from the network to stop the spreading of the disease.

325 *Random sampling*

326 In case of random sampling, testing (and consequent removing of SARS-CoV-2 positive people from
327 the contact network), the critical immunization g_c can be defined as:

$$328 \quad g_c = 1 - \frac{\lambda_c}{\lambda} \quad (5)$$

329 Besides random sampling, there are other options as well, stemming from the characteristic of the
330 scale free networks first described as the error tolerance of networks (65). If we remove the nodes
331 from a network in a targeted manner, the spreading on the network could be quickly slowed down or

332 stopped. As it was demonstrated, the rapid spread of diseases is caused by the fact that there is a large
333 variance in the degrees of the nodes in these networks ($\langle k^2 \rangle \gg \langle k \rangle$), and this comes from the
334 presence of hubs. If we want to decrease the variance (thus increasing λ_c), we have to block hubs
335 from interacting.

336 *Selective sampling*

337 If we don't know the exact mapping of the contact network, we could reach for the 'friendship
338 paradox' (66) and the immunization strategy based on it proposed by Cohen et al. (67). The
339 friendship paradox says that on average the neighbours of a node have higher degrees than the node
340 itself. The average degree of a node's neighbour doesn't equal to $\langle k \rangle$, but it is a different number,
341 depending largely also on $\langle k^2 \rangle$ (25). The origin of this phenomenon is that it is more likely for a
342 random node to be connected to a hub than to a small degree node, because hubs have more
343 connections than other nodes. Thus, immunizing (or isolating) the contacts of randomly selected
344 individuals, we target the hubs without knowing exactly which individuals are the hubs.

345 *Targeted sampling*

346 If we knew the whole contact network, we could target the most prominent hubs. We don't know the
347 exact mapping of the Hungarian social network, but we can have the following assumptions:

- 348 - The network is scale-free;
- 349 - where the probability p_k that a node has exactly k links is: $p_k = \frac{k^{-\gamma}}{\xi(\gamma)}$, where γ is the degree
350 exponent and $\xi(\gamma)$ is the Riemann-zeta function (using discrete formalism (25));
- 351 - and $2 < \gamma < 3$, as in most of real-life networks.

352 With targeted sampling we try to remove all nodes whose degree is larger than k_t . From an
353 epidemiological viewpoint this is the same as removing the high degree nodes from the network with
354 their links as well. With this intervention, the network will change, and λ_c will increase (25):

$$355 \quad \lambda'_c = \left[\frac{\gamma-2}{3-\gamma} k_t^{3-\gamma} k_{min}^{\gamma-2} - \frac{\gamma-2}{3-\gamma} k_t^{5-2\gamma} k_{min}^{2\gamma-4} + k_t^{2-\gamma} k_{min}^{\gamma-2} - 1 \right]^{-1} \quad (6)$$

356 Depending on the degree exponent, and setting k_{min} to 1, we could obtain target degrees (k_t) with the
357 new epidemic thresholds (λ'_c).

358

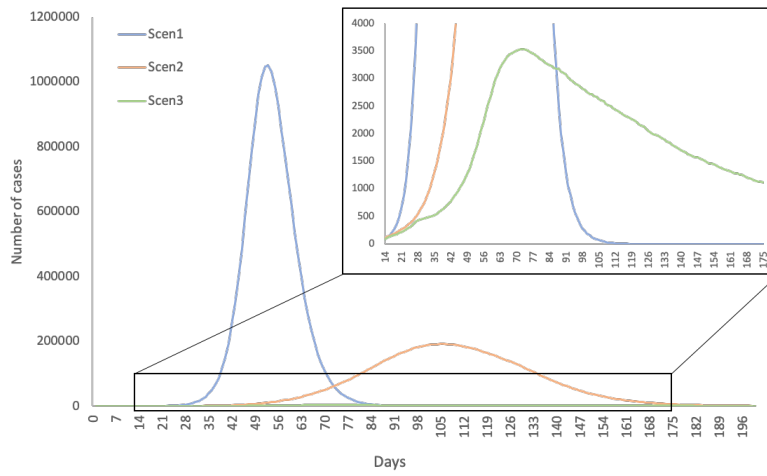
359 **Results**

360 **Results of epidemiological modelling**

361 Different scenarios were run in the publicly available version of GLEAMviz software with the
362 settings described in 'Methods' section. As the software only provides the number and cumulative
363 number of new transitions of individuals per 1000 people regarding one compartment to another in a
364 daily breakdown, an algorithm was developed in KNIME software (63) in order to automatically
365 convert the GLEAMviz outputs into actual daily case numbers of different compartments.

366 Figures 2 and 3 show the comparison of distribution of Infected and Exposed (latent) individuals in
 367 different scenarios.

368 **Figure 2**



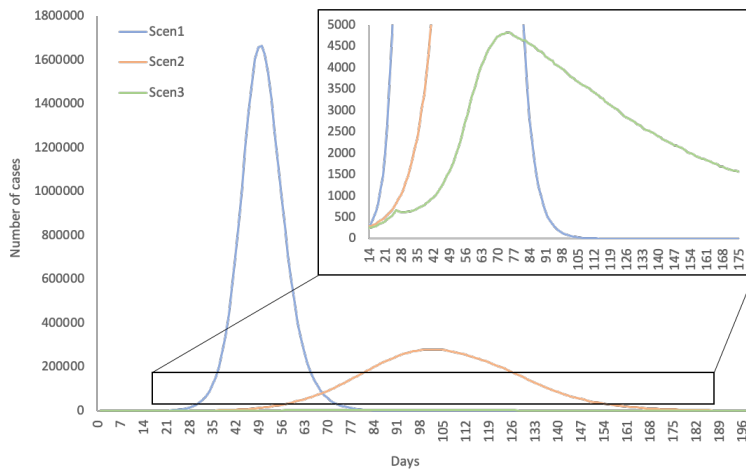
Distribution of Infected individuals in *Scenarios 1 to 3*

369
 370

371

372

Figure 3



Distribution of Exposed (latent) individuals in *Scenarios 1 to 3*.

373

374

375 The proportion of maximally affected latent and infected people (daily and overall) can be seen in
 376 Table 5. According to the modelling, about 1,000,000; 190,000 and 3,500 people will be infected on
 377 the day, when the epidemic reaches its peak in *Scenarios 1, 2 and 3*, respectively. Overall, about
 378 5,400,000; 3,300,000 and 110,000 people will get through the infection with moderate or serious
 379 symptoms in *Scenarios 1, 2 and 3* and respectively. Note that in case of Scenario 3, the maximum
 380 number was not reached till the end of the simulation (365 days, which was the limitation of the
 381 software).

382 Table 5. Proportion of maximum number of daily and cumulated cases of infected and latent people
 383 in Hungary.

			Proportion in the population¹ (median with LCL² and UCL³) (%)	No. of days⁴
Scenario 1	Maximum of daily cases	Infected	11.42 (7.99-12.62)	52
		Latent	18.07 (12.51-20.29)	49
	Maximum of cumulated cases	Infected	58.69 (58.65-58.72)	118
		Latent	93.89 (93.85-93.91)	122
Scenario 2	Maximum of daily cases	Infected	2.08 (1.76-2.38)	105
		Latent	3.05 (2.57-3.05)	101
	Maximum of cumulated cases	Infected	35.89 (35.82-35.94)	268
		Latent	57.36 (57.26-57.42)	279
Scenario 3	Maximum of daily cases	Infected	0.04 (0.04-0.04)	72
		Latent	0.05 (0.05-0.06)	74
	Maximum of cumulated cases	Infected	1.22 (1.12-1.31)	365*
		Latent	1.85 (1.69-2.00)	365*

384 as 9,213,366 people

385 ²: Lower confidence limit originating from the 20 different simulations

386 ³: Upper confidence limit originating from the 20 different simulations

387 ⁴: Regarding median value

388 *: Maximum number was not reached till the end of the simulation (365 days, which was the limitation of the software)

389

390 Regarding exposed (latent) people, who will only have mild symptoms or no symptoms at all
 391 (according to our assumption), on the day of the peak of the epidemic, about 1,700,000; 280,000 and
 392 4,800 people will be affected in *Scenarios 1, 2 and 3*, respectively. Overall, about 8,700,000;
 393 5,300,000 and 170,000 people will get through the infection with mild symptoms or as asymptomatic
 394 cases in *Scenarios 1, 2 and 3*, respectively. The same limitation in case of Scenario 3 applies here as
 395 well regarding the maximum number of latent people.

396 Note that the modelling is a robust estimate for actual case numbers, therefore only approximate
 397 values are indicated.

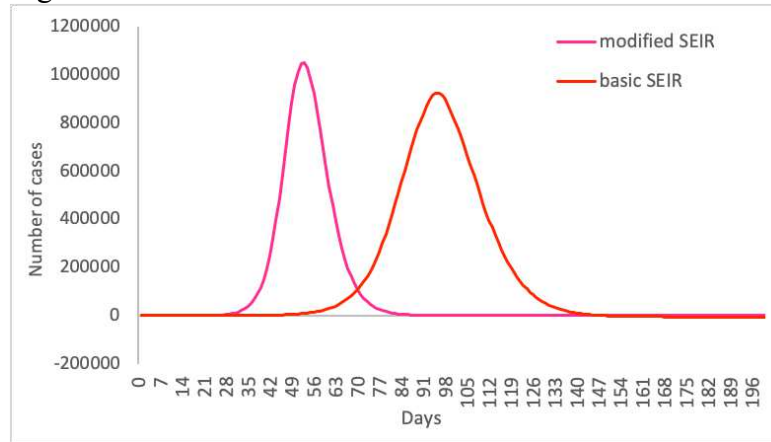
398

399 **Comparison of modified SEIR model with traditional SEIR model**

400 Basic SEIR model results in somewhat lower number of daily infections, daily latent cases, and
 401 cumulative latent cases (1.38%, 3.07%, and 1.74%, respectively) but overall, the cumulative number
 402 of infectious individuals are 33.47% higher compared to the modified SEIR model (Table 6). It can
 403 be seen that the peak of the curve is shifted in the basic SEIR model (from about 50 days after the
 404 start date of the simulation to the ~90th day) (Fig. 4.).

405

Figure 4



Comparison of the distribution of Infected individuals in case of modified SEIR model and basic SEIR model in case of *Scenario 1*

406

407

408

409

410 Table 6. Proportion of maximum number of daily and cumulated cases of infected and latent people
411 in modified SEIR model compared with basic SEIR model Settings of Scenario 1 was applied.

		Modified SEIR model		Basic SEIR model	
		Proportion in the population ¹ (median with LCL ² and UCL ³) (%)	No. of days ⁴	Proportion in the population ¹ (median with LCL ² and UCL ³) (%)	No. of days ⁴
Maximum no. of daily cases	Infected	11.42 (7.99-12.62)	52	10.04 (8.01-10.89)	95
	Latent	18.07 (12.51-20.29)	49	15.00 (11.61-16.68)	91
Maximum no. of cumulated cases	Infected	58.69 (58.65-58.72)	118	92.16 (92.10-92.22)	214
	Latent	93.89 (93.85-93.91)	122	92.15 (92.10-92.20)	211

412 ¹: Population of Hungary registered in GLEAMviz was 9,213,366 people

413 ²: Lower confidence limit originating from the 20 different simulations

414 ³: Upper confidence limit originating from the 20 different simulations

415 ⁴: Regarding median value

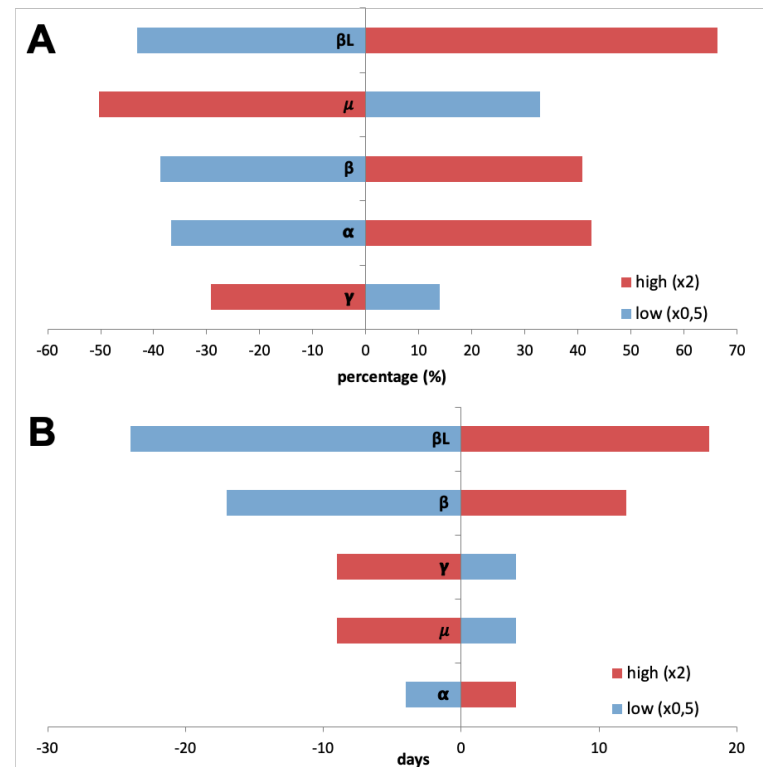
416

417 **Sensitivity analysis of modified SEIR model**

418

419 Most pronounced changes in both chosen endpoints can be seen in case of β_L , increasing its value by
420 2 times resulted in a ~66% increase in the number of maximum daily infections (Fig. 5A), and
421 decreasing its value to the half of the original ended up in a 24 days sooner peak in the curve of the
422 number of daily infections (Fig. 5B). However, other the importance of parameters such as μ and β
423 are also indicated by the tornado-plot.

Figure 5



Results of sensitivity analysis of the modified SEIR model: changes in daily maximum value of individuals in the infected compartment (A) and changes in the number of the days related to the former endpoint (B)

425
426
427
428

429

430 Results of network analysis

431 To address the problem caused by the inability of conventional compartment models to capture the
432 non-homogenous nature of the population, network-based analyses were also performed, which
433 yielded the following results.

434 Based on the Copenhagen Networks Study (60) data, we found average degree $\langle k \rangle = 46$, the second
435 moment of the degree $\langle k^2 \rangle = 2847$ and based on Equation (4) the epidemic threshold $\lambda_c = 0.016$. Basic
436 parameters of modified SEIR model (*Scenario 1*) was set to be in line with the average R_0 value of
437 3.1 of Read et al. (32) and Tian et al. (33). Using Equation (3), the spreading rate of the virus was
438 $\lambda = 0.067$, which means that for stopping the epidemic, we need to change the network in such a way
439 that λ_c will be increased above this value.

440 *Random sampling*

441 In case of random sampling, testing (and consequent removing of SARS-CoV-2 positive people from
442 the contact network), based on equation (5) we have found the critical immunization to be $g_c = 0.761$.
443 This means that 76.1% of the population shall be removed from the network. This implies very strict
444 sampling and quarantine measures with testing a very large proportion of the population.

445 *Selective sampling*

446 Using the ‘friendship paradox’, the procedure proposed by Cohen et al. (67), consists of three steps:

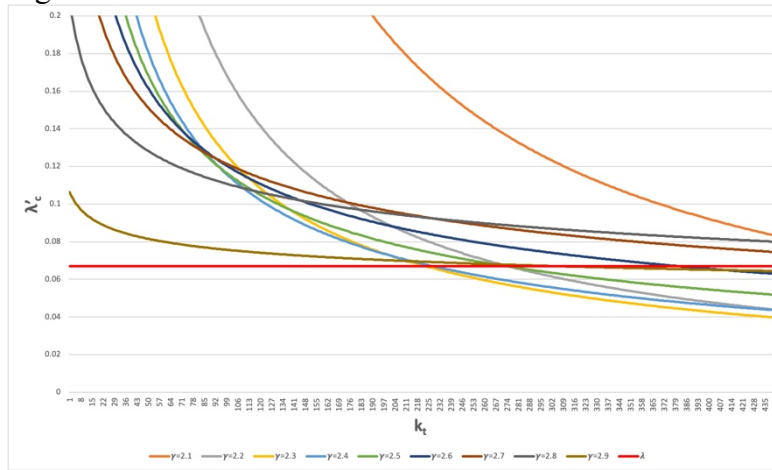
- 447 1. Choosing randomly a fraction of nodes, this is layer 0.
- 448 2. Selecting randomly a link for each node in layer 0. The nodes to which these links connect will
- 449 form layer 1.
- 450 3. Immunizing (in our case sampling and testing) the layer 1 individuals.

451 This sampling strategy doesn’t require information on the structure of the network. According to
 452 Cohen et al. (67), g_c is systematically under 0.3. It means that by selecting and removing a randomly
 453 chosen neighbour of 30% of the population, the spreading of the disease could be stopped. With
 454 selecting contacts referred simultaneously by more people, this strategy could be even enhanced.

455 *Targeted sampling*

456 With targeted sampling we try to remove all nodes whose degree is larger than k_t . Based on equation
 457 (6), we could obtain target degrees (k_t) with the new epidemic thresholds (λ'_c) which are presented on
 458 Figure 6. The figure shows target degrees k_t in the range of 234 (for $\gamma=2.3$) to >1000 (for $\gamma=2.8$),
 459 meaning that if we could sample (and then contain all positive cases) the super-spreaders with contact
 460 number above 234, the epidemic threshold would be high enough to stop the disease.

461 **Figure 6**



462 Epidemic thresholds (λ'_c) of different degree exponents (γ) and target
 463 degrees (k_t) calculated to increase the epidemic threshold above the
 464 spreading rate of COVID-19 with targeted sampling. The spreading rate
 465 (λ) of the virus is set to 0.067 (red line).
 466

467 How does it translate to the Hungarian population? Idealizing a scale-free network, the number of
 468 people with contacts $k \geq k_t$ can be calculated with (25):

469
$$N_{k \geq k_t} = N \sum_{k=k_t}^{\infty} \frac{k^{-\gamma}}{\xi(\gamma)} \quad (8)$$

470 Setting $\gamma=2.3$ and $k_t=234$, this is in the magnitude of 0.04% of the population only.

471

472 **Discussion**

473

474 **Potentials and limitations of the modelling**

475 Scenarios have been designed to simulate the most likely spread of COVID-19 in Hungary with no
476 interventions (*Scenario 1*) and the effect of actually applied interventions (*Scenarios 2 and 3*) in
477 order to gain information on the effect of intervention measures on the disease spreading. According
478 to the results, the applied interventions (social distancing and hygienic measures) have a great impact
479 on the disease spreading and are effective in controlling the COVID-19 epidemic (*Scenario 3*).

480 The main advantage of epidemiological modelling with GLEAMviz software is that besides the
481 characteristic parameters of the infectious disease, other essential factors are taken into account when
482 simulating the disease spreading, namely population density and mobility of the population. The
483 irregular network structure, that affects the local spread of infectious disease between neighbouring
484 subpopulations is captured in GLEAMviz datasets, so as the difference between high traffic and low
485 traffic airports that has a significant impact of disease spreading around the globe.

486 Simulations are evaluated for the Hungarian region, but with GLEAMviz, it is possible to set the
487 initial number of infected individuals in different cities on the day when the simulation starts, thereby
488 the impact of global presence of infected people is also taken into account. Note that registered
489 number of infected people in different countries/cities carries bias as the protocol for registering
490 COVID-19 positive cases and number of tests performed differ greatly from country to country.
491 Nonetheless, these data and this option provide additional adjustable settings that contributes to more
492 realistic simulations.

493 **Evaluation of modified SEIR model – sensitivity analysis**

494 All modelling has their limitations, and this applies particularly to modelling of emerging diseases
495 such as COVID-19. As limited data are available regarding SARS-CoV-2 and the spread of COVID-
496 19, parameters of the compartment model can only be estimated. Our modified SEIR model has been
497 made by using available data from scientific literature regarding the compartment model parameters
498 and its novelty is that the route of infection transmission from the Exposed compartment (latent
499 individuals) is built in. Compared to the traditionally applied SEIR model, in which latent individuals
500 cannot transmit the infection to susceptible people, it results in an earlier and higher peak in the
501 epidemic curve of infected individuals, which means a faster epidemic course with more infected
502 people in shorter period of time, that poses greater burden to the healthcare system. However, total
503 number of infections are lower altogether in the modified model compared to the basic SEIR model.
504 According to this result, the experienced characteristics of COVID-19 epidemics, namely the so-
505 called ‘exponential growth’ of the disease spread can be explained by the disease transmission of
506 latent people in case of SARS-CoV-2. Sensitivity analysis of the modified SEIR model also reveals
507 the importance of the disease transmission by latent individuals. According to the results, disease
508 transmission related to latent individuals has the greatest impact on the results of the simulation
509 regarding the number of maximum daily infections and the time of the peak of the epidemic.

510 **Evaluation of network analysis results**

511 When taking into account the social contact network topology during intervention planning, we have
512 to be aware of the specific challenges and also opportunities these network characteristics pose. Most
513 of the counterintuitive network phenomena are caused by the presence of hubs, i.e. nodes with large
514 amount of contacts, which could also be identified as super-spreaders. One of the results is that the
515 diseases spread much faster on real networks than conventional compartment models would predict.
516 This also means that the R_0 identified as a benchmark value might be wrong: even if $R_0 < 1$, there

517 might be still nodes in the network whose degree is higher than the average degree, maintaining and
518 spreading the disease.

519 The usual intervention strategies mentioned in this paper are still useful and effective, but they don't
520 target the super-spreader hubs. When planning sampling strategies, *random sampling* would imply
521 very strict sampling and quarantine measures with testing a very large proportion of the population
522 (>75%). When the 'friendship paradox' (i.e. on average the neighbours of a node have higher degree
523 than the node itself) would be used for planning *selective sampling*, a significantly lower number of
524 samples (~30%) would suffice. And if we could find the super-spreader hubs in a network during
525 *targeted sampling*, <1% of the population would be enough to be sampled, tested and isolated.

526 Of course, natural contact networks are not ideal scale-free networks, and we don't know the exact
527 super-spreaders either. Nevertheless, according to the recent analysis of the Hungarian Centre for
528 Economic and Regional Studies Institute of Economics on occupations affected the most by the
529 COVID-19 outbreak (69) 18% of the people are working in these occupational areas. These include
530 healthcare and social workers, retail and restaurant workers, drivers, cleaning staff, pharmacists,
531 veterinarians, public transport workers, postmen and waste removal staff. If the targeted sampling
532 strategy would aim for these occupations, with strict quarantine measures of the positive cases, the
533 spreading of the virus could be significantly slowed down.

534 **Conclusion**

535 **Comparison with real COVID-19 epidemiological situation in Hungary**

536 The first wave of the disease spreading, according to the reported COVID-19 cases in Hungary,
537 SARS-CoV-2 have not caused a great epidemic in Hungary Multiple reasons can explain this, some
538 of them are listed hereunder.

- 539 • By the time the epidemic reached Hungary, there were several frightening scenarios (massive
540 amount of infections and deaths caused by COVID-19 in China, Italy etc.) that warned the
541 public and raised the awareness for caution about COVID-19 and discipline regarding social
542 distancing and hygiene. People have started to draw each other's attention through social
543 media and encouraged staying at home, therefore social distancing have started even earlier
544 and have been applied stricter than the actual measurements of the Hungarian government
545 required.
- 546 • Because of conscious social distancing, super-spreading events have been prevented in the
547 very early phase of the epidemic, which has a great impact on the fate of later number of
548 infections (59).
- 549 • Many studies investigate the association of Bacillus Calmette-Guérin (BCG) vaccination with
550 reduced morbidity and mortality of COVID-19 (70,71). In Hungary, BCG vaccination is
551 compulsory since 1954, therefore BCG vaccination coverage is very high. This can also
552 contribute to the low number of COVID-19 infections in Hungary.

553 Our modelling results show a good correlation with the results of the Hungarian CoronaVirus
554 disease-19 Epidemiological Research(72). H-UNCOVER was a large-scale, cross-sectional,
555 representative population screening of Hungarian male or female patients aged 14 and over who live
556 in private households, aiming for sampling and investigating the rate of the infected patients,
557 asymptomatic carrier and healed patients (48). According of the extrapolation of the results of 10,575

558 patients sampled between 1-16 May 2020, there were 2,421 active cases in Hungary and 56,439
559 people were asymptomatic carriers and healed patients.

560 According to the results of our modelling in *Scenario 3*, there were 3,527 active infected cases on day
561 70 (12th May) and 38,692 cumulative recovered people by day 70 and 4,756 active latent cases on
562 day 70, adding up to 43,448 asymptomatic carriers and healed patients.

563

564 **Proposal for disease control with agile, risk-based testing**

565 Our study proposes a long-term feasible risk-based approach for testing SARS-CoV-2 infections, that
566 could gradually replace isolation interventions by the early detection of positive cases between the
567 so-called 'super-spreaders', thereby preventing mass infections and breaking infection chains with
568 removing the seed of the infection in a timely manner. In cases when number of positive cases tend
569 to increase nonetheless of the quarantine of affected people, social isolation measures can be re-
570 initiated in a timely manner and epidemic crisis can thereby be prevented.

571 With the help of network analysis, people can be grouped into risk categories regarding SARS-CoV-
572 2 transmission. In this case, the key parameter for establishing risk categories is the number of
573 physical interactions between people. A continuous testing is suggested but with the allocation of
574 resources (test kits, testing personnel, financial resources) to the high-risk groups. People could be
575 categorized by risk scores of physical interactions based on their occupation. Occupations like
576 healthcare and social workers, retail and restaurant workers, drivers, cleaning staff, pharmacists,
577 veterinarians, public transport workers, postmen and waste removal staff would fall into this high-
578 risk group. These people must be tested much more often as they play key role in SARS-CoV-2
579 transmission. From this group, healthcare workers could be identified as key actors from network
580 perspective, implying even stricter sampling and testing regime for them. When identified positive
581 cases of super-spreaders would be isolated, this would have a large effect on the contact network
582 itself, cutting off all the links of the large hubs, thus slowing down the spreading considerably.

583 Our approach is generally applicable for the prevention and early detection of epidemics caused by
584 other microorganisms as well, thereby protecting human health and preventing economic crises
585 caused by emerging and re-emerging diseases.

586 **Proposal for data collection and data sharing**

587 Our study also points to the well-known fact that models are only as good as their input data. When
588 modelling and planning intervention strategies, fit-for-purpose and timely data are essential. Using
589 specific population like college student data can't be used for precise modelling of the spreading of
590 diseases in other societal groups. Unfortunately, there is a lack of social contact data with sufficient
591 granularity, and advances on network science couldn't be fully exploited in real-life situations. It is
592 not to say that collecting and sharing contact network data for public health purposes would
593 overwrite data protection and privacy aspects, but as Oliver et al. (73) pointed out, there are available
594 data sources like mobile phone data, which could be extremely useful for such purposes. These
595 datasets, if would be made available in a careful and transparent manner and taking into account data
596 protections issues, could also be used for other important public health domains, like foodborne
597 disease outbreak investigation.

598 In our paper we had two important objectives regarding network analysis approach to
599 epidemiological modelling:

- 600 - Showing the profound implications of network theory for epidemiological modelling and risk
601 management, since the network epidemiological approach is not widely known in the public
602 health community. Most of the analyses and also intervention strategies don't take into
603 account the inhomogeneity of the connections nor the network-based background of the
604 spreading of the virus. Even when there is a general knowledge on the role of super-spreaders,
605 the quantification of this role is not well known.
- 606 - Network analysis (but also all computational science methods) need large amount of good
607 quality data and the spread of these methods could be supported by easy-to-use tools. We
608 wanted to raise awareness also on this issue.

609 These two objectives are in close connection, since the lack of fit-for-purpose data and access to
610 computational methods prevent the public health community from applying network-based approach
611 in the decision-making process. However, the public health community should work towards solving
612 data and tool related issues, for example with using proxy data in a short term (e.g. mobile phone
613 data, tracing applications, etc.) or with planned exercises on network data collection in the long run.

614

615 **Declaration**

616 Ethics approval and consent to participate
617 Not applicable.

618
619 Consent for publication
620 The authors consent for publication.

621
622 Availability of data and materials
623 All the analysed and generated data during this study are included and referred in this published
624 article. The KNIME workflow is available at [https://univet.hu/en/research/dfi/publications/scientific-
625 publications/covid-19/](https://univet.hu/en/research/dfi/publications/scientific-publications/covid-19/).

626
627 Competing interests
628 The authors declare no competing interests.

629
630 Funding
631 Not applicable.

632
633 Author Contributions
634 ZSF prepared the modelling and wrote the main body of the text; ÁJ created the concept of the
635 network study and prepared the related research; TE and ZSF prepared the tables; SZCS prepared the
636 figures; MS, EO, SZCS, TE and ZSF did the literature research; MS reviewed the first draft of the
637 manuscript. TE prepared the sensitivity analysis. All authors contributed to the creation of the
638 epidemiological compartment model in the study and the concept of the research. All authors
639 contributed to manuscript revision, read and approved the version to be submitted

640

641 Acknowledgement
642 Not applicable.

643 **References**

- 644 1. Zhou P, Yang X-L, Wang X-G, Hu B, Z. hang L, Zhang W, et al. A pneumonia outbreak
645 associated with a new coronavirus of probable bat origin. *Nature*. 2020 Mar 12;579(7798):270–3.
- 646 2. Zheng J. SARS-CoV-2: an Emerging Coronavirus that Causes a Global Threat. *Int J Biol Sci*.
647 2020;16(10):1678–85.
- 648 3. Coronaviridae Study Group of the International Committee on Taxonomy of Viruses. The species
649 Severe acute respiratory syndrome-related coronavirus: classifying 2019-nCoV and naming it
650 SARS-CoV-2. *Nat Microbiol*. 2020 Apr;5(4):536–44.
- 651 4. WHO. Naming the coronavirus disease (COVID-19) and the virus that causes it [Internet]. 2020.
652 Available from: [https://www.who.int/emergencies/diseases/novel-coronavirus-2019/technical-](https://www.who.int/emergencies/diseases/novel-coronavirus-2019/technical-guidance/naming-the-coronavirus-disease-(covid-2019)-and-the-virus-that-causes-it)
653 [guidance/naming-the-coronavirus-disease-\(covid-2019\)-and-the-virus-that-causes-it](https://www.who.int/emergencies/diseases/novel-coronavirus-2019/technical-guidance/naming-the-coronavirus-disease-(covid-2019)-and-the-virus-that-causes-it)
- 654 5. Singhal T. A Review of Coronavirus Disease-2019 (COVID-19). *Indian J Pediatr*. 2020
655 Apr;87(4):281–6.
- 656 6. Cascella M, Rajnik M, Cuomo A, Dulebohn SC, Di Napoli R. Features, Evaluation, and
657 Treatment of Coronavirus. In: *StatPearls* [Internet]. Treasure Island (FL): StatPearls Publishing;
658 2020 [cited 2020 Nov 25]. Available from: <http://www.ncbi.nlm.nih.gov/books/NBK554776/>
- 659 7. van Doremalen N, Bushmaker T, Morris DH, Holbrook MG, Gamble A, Williamson BN, et al.
660 Aerosol and surface stability of HCoV-19 (SARS-CoV-2) compared to SARS-CoV-1 [Internet].
661 *Infectious Diseases (except HIV/AIDS)*; 2020 Mar [cited 2020 Nov 25]. Available from:
662 <http://medrxiv.org/lookup/doi/10.1101/2020.03.09.20033217>
- 663 8. Cai J, Sun W, Huang J, Gamber M, Wu J, He G. Indirect Virus Transmission in Cluster of
664 COVID-19 Cases, Wenzhou, China, 2020. *Emerg Infect Dis*. 2020 Jun;26(6):1343–5.
- 665 9. Jia J, Ding J, Liu S, Liao G, Li J, Duan B, et al. Modeling the Control of COVID-19: Impact of
666 Policy Interventions and Meteorological Factors. *arXiv:200302985 [math, q-bio]* [Internet]. 2020
667 Mar 5 [cited 2020 Nov 25]; Available from: <http://arxiv.org/abs/2003.02985>
- 668 10. Koo JR, Cook AR, Park M, Sun Y, Sun H, Lim JT, et al. Interventions to mitigate early spread of
669 SARS-CoV-2 in Singapore: a modelling study. *The Lancet Infectious Diseases*. 2020
670 Jun;20(6):678–88.
- 671 11. Peng L, Yang W, Zhang D, Zhuge C, Hong L. Epidemic analysis of COVID-19 in China by
672 dynamical modeling [Internet]. *Epidemiology*; 2020 Feb [cited 2020 Nov 25]. Available from:
673 <http://medrxiv.org/lookup/doi/10.1101/2020.02.16.20023465>
- 674 12. Shen M, Peng Z, Xiao Y, Zhang L. Modeling the Epidemic Trend of the 2019 Novel Coronavirus
675 Outbreak in China. *The Innovation*. 2020 Nov;1(3):100048.

- 676 13. Li D, Liu Z, Liu Q, Gao Z, Zhu J, Yang J, et al. Estimating the Efficacy of Quarantine and
677 Traffic Blockage for the Epidemic Caused by 2019-nCoV (COVID-19):A Simulation Analysis
678 [Internet]. *Epidemiology*; 2020 Feb [cited 2020 Nov 25]. Available from:
679 <http://medrxiv.org/lookup/doi/10.1101/2020.02.14.20022913>
- 680 14. Peak CM, Kahn R, Grad YH, Childs LM, Li R, Lipsitch M, et al. Modeling the Comparative
681 Impact of Individual Quarantine vs. Active Monitoring of Contacts for the Mitigation of COVID-
682 19 [Internet]. *Infectious Diseases (except HIV/AIDS)*; 2020 Mar [cited 2020 Nov 25]. Available
683 from: <http://medrxiv.org/lookup/doi/10.1101/2020.03.05.20031088>
- 684 15. Ferguson N, Laydon D, Nedjati Gilani G, Imai N, Ainslie K, Baguelin M, et al. Report 9: Impact
685 of non-pharmaceutical interventions (NPIs) to reduce COVID19 mortality and healthcare
686 demand [Internet]. Imperial College London; 2020 Mar [cited 2020 Nov 25]. Available from:
687 <http://spiral.imperial.ac.uk/handle/10044/1/77482>
- 688 16. Tang Z, Li X, Li H. Prediction of New Coronavirus Infection Based on a Modified SEIR Model.
689 *medRxiv* [Internet]. 2020 Mar 6; Available from:
690 <https://www.medrxiv.org/content/10.1101/2020.03.03.20030858v1>
- 691 17. Flaxman S, Mishra S, Gandy A, Unwin H, Coupland H, Mellan T, et al. Report 13: Estimating
692 the number of infections and the impact of non-pharmaceutical interventions on COVID-19 in 11
693 European countries [Internet]. Imperial College London; 2020 Mar [cited 2020 Nov 25].
694 Available from: <http://spiral.imperial.ac.uk/handle/10044/1/77731>
- 695 18. Wu JT, Leung K, Leung GM. Nowcasting and forecasting the potential domestic and
696 international spread of the 2019-nCoV outbreak originating in Wuhan, China: a modelling study.
697 *Lancet*. 2020 Jan 31;395:689–97.
- 698 19. Li R, Pei S, Chen B, Song Y, Zhang T, Yang W, et al. Substantial undocumented infection
699 facilitates the rapid dissemination of novel coronavirus (SARS-CoV-2). *Science*. 2020 May
700 1;368(6490):489–93.
- 701 20. Mizumoto K, Kagaya K, Zarebski A, Chowell G. Estimating the asymptomatic proportion of
702 coronavirus disease 2019 (COVID-19) cases on board the Diamond Princess cruise ship,
703 Yokohama, Japan, 2020. *Eurosurveillance* [Internet]. 2020 Mar 12 [cited 2020 Nov 25];25(10).
704 Available from: [https://www.eurosurveillance.org/content/10.2807/1560-](https://www.eurosurveillance.org/content/10.2807/1560-7917.ES.2020.25.10.2000180)
705 [7917.ES.2020.25.10.2000180](https://www.eurosurveillance.org/content/10.2807/1560-7917.ES.2020.25.10.2000180)
- 706 21. Nishiura H, Kobayashi T, Miyama T, Suzuki A, Jung S-M, Hayashi K, et al. Estimation of the
707 asymptomatic ratio of novel coronavirus infections (COVID-19). *Int J Infect Dis*. 2020;94:154–5.
- 708 22. Du Z, Xu X, Wu Y, Wang L, Cowling BJ, Meyers LA. Serial Interval of COVID-19 among
709 Publicly Reported Confirmed Cases. *Emerg Infect Dis*. 2020 Jun;26(6):1341–3.
- 710 23. Ganyani T, Kremer C, Chen D, Torneri A, Faes C, Wallinga J, et al. Estimating the generation
711 interval for coronavirus disease (COVID-19) based on symptom onset data, March 2020.
712 *Eurosurveillance* [Internet]. 2020 Apr 30 [cited 2020 Nov 25];25(17). Available from:
713 <https://www.eurosurveillance.org/content/10.2807/1560-7917.ES.2020.25.17.2000257>

- 714 24. Chisholm RH, Campbell PT, Wu Y, Tong SYC, McVernon J, Geard N. Implications of
715 asymptomatic carriers for infectious disease transmission and control. *R Soc open sci.* 2018
716 Feb;5(2):172341.
- 717 25. Barabási A-L, Pósfai M. *Network science.* Cambridge, United Kingdom: Cambridge University
718 Press; 2016. 456 p.
- 719 26. WHO. Statement on the first meeting of the International Health Regulations (2005) Emergency
720 Committee regarding the outbreak of novel coronavirus (2019-nCoV) [Internet]. 2020. Available
721 from: [https://www.who.int/news/item/23-01-2020-statement-on-the-meeting-of-the-international-](https://www.who.int/news/item/23-01-2020-statement-on-the-meeting-of-the-international-health-regulations-(2005)-emergency-committee-regarding-the-outbreak-of-novel-coronavirus-(2019-ncov))
722 [health-regulations-\(2005\)-emergency-committee-regarding-the-outbreak-of-novel-coronavirus-](https://www.who.int/news/item/23-01-2020-statement-on-the-meeting-of-the-international-health-regulations-(2005)-emergency-committee-regarding-the-outbreak-of-novel-coronavirus-(2019-ncov))
723 [health-regulations-\(2005\)-emergency-committee-regarding-the-outbreak-of-novel-coronavirus-](https://www.who.int/news/item/23-01-2020-statement-on-the-meeting-of-the-international-health-regulations-(2005)-emergency-committee-regarding-the-outbreak-of-novel-coronavirus-(2019-ncov))
(2019-ncov)
- 724 27. Tang B, Wang X, Li Q, Bragazzi NL, Tang S, Xiao Y, et al. Estimation of the Transmission Risk
725 of the 2019-nCoV and Its Implication for Public Health Interventions. *JCM.* 2020 Feb
726 7;9(2):462.
- 727 28. Liu T, Hu J, Xiao J, He G, Kang M, Rong Z, et al. Time-varying transmission dynamics of Novel
728 Coronavirus Pneumonia in China [Internet]. *Systems Biology*; 2020 Jan [cited 2020 Nov 25].
729 Available from: <http://biorxiv.org/lookup/doi/10.1101/2020.01.25.919787>
- 730 29. Li Q, Guan X, Wu P, Wang X, Zhou L, Tong Y, et al. Early Transmission Dynamics in Wuhan,
731 China, of Novel Coronavirus–Infected Pneumonia. *N Engl J Med.* 2020 Mar 26;382(13):1199–
732 207.
- 733 30. Linton NM, Kobayashi T, Yang Y, Hayashi K, Akhmetzhanov AR, Jung S-M, et al. Incubation
734 Period and Other Epidemiological Characteristics of 2019 Novel Coronavirus Infections with
735 Right Truncation: A Statistical Analysis of Publicly Available Case Data. *J Clin Med.* 2020 Feb
736 17;9(2).
- 737 31. Lauer SA, Grantz KH, Bi Q, Jones FK, Zheng Q, Meredith HR, et al. The Incubation Period of
738 Coronavirus Disease 2019 (COVID-19) From Publicly Reported Confirmed Cases: Estimation
739 and Application. *Annals of Internal Medicine.* 2020 May 5;172(9):577–82.
- 740 32. Read JM, Bridgen JRE, Cummings DAT, Ho A, Jewell CP. Novel coronavirus 2019-nCoV: early
741 estimation of epidemiological parameters and epidemic predictions [Internet]. *Infectious*
742 *Diseases (except HIV/AIDS)*; 2020 Jan [cited 2020 Nov 25]. Available from:
743 <http://medrxiv.org/lookup/doi/10.1101/2020.01.23.20018549>
- 744 33. Tian H, Liu Y, Li Y, Wu C-H, Chen B, Kraemer MUG, et al. An investigation of transmission
745 control measures during the first 50 days of the COVID-19 epidemic in China. *Science.* 2020
746 May 8;368(6491):638–42.
- 747 34. Patrozou E, Mermel LA. Does Influenza Transmission Occur from Asymptomatic Infection or
748 Prior to Symptom Onset? *Public Health Rep.* 2009 Mar;124(2):193–6.
- 749 35. Longini IM. Containing Pandemic Influenza with Antiviral Agents. *American Journal of*
750 *Epidemiology.* 2004 Apr 1;159(7):623–33.
- 751 36. GLEAMviz [Internet]. Available from: <http://www.gleamviz.org>

- 752 37. Broeck WV den, Gioannini C, Gonçalves B, Quaggiotto M, Colizza V, Vespignani A. The
753 GLEaMviz computational tool, a publicly available software to explore realistic epidemic
754 spreading scenarios at the global scale. *BMC Infect Dis.* 2011 Dec;11(1):37.
- 755 38. Balcan D, Hu H, Goncalves B, Bajardi P, Poletto C, Ramasco JJ, et al. Seasonal transmission
756 potential and activity peaks of the new influenza A(H1N1): a Monte Carlo likelihood analysis
757 based on human mobility. *BMC Med.* 2009 Dec;7(1):45.
- 758 39. Balcan D, Gonçalves B, Hu H, Ramasco JJ, Colizza V, Vespignani A. Modeling the spatial
759 spread of infectious diseases: The GLObal Epidemic and Mobility computational model. *Journal*
760 *of Computational Science.* 2010 Aug;1(3):132–45.
- 761 40. Balcan D, Colizza V, Goncalves B, Hu H, Ramasco JJ, Vespignani A. Multiscale mobility
762 networks and the spatial spreading of infectious diseases. *Proceedings of the National Academy*
763 *of Sciences.* 2009 Dec 22;106(51):21484–9.
- 764 41. Simini F, González MC, Maritan A, Barabási A-L. A universal model for mobility and migration
765 patterns. *Nature.* 2012 Apr;484(7392):96–100.
- 766 42. Google. Community Mobility Reports [Internet]. Google; 2020. Available from:
767 <https://www.google.com/covid19/mobility/>
- 768 43. Waze. Waze Stats: Active Wazers in HU Budapest. [Internet]. Available from:
769 <http://wazestats.com/active.php?city=7>
- 770 44. COVID-19 pandemic in Hungary [Internet]. Available from: koronavirus.gov.hu
- 771 45. OAG. Coronavirus airline schedules data. [Internet]. Official Aviation Guide; 2020. Available
772 from: <https://www.oag.com/coronavirus-airline-schedules-data>
- 773 46. Ren Y, Ercsey-Ravasz M, Wang P, González MC, Toroczkai Z. Predicting commuter flows in
774 spatial networks using a radiation model based on temporal ranges. *Nat Commun.* 2014
775 Dec;5(1):5347.
- 776 47. Monto AS, DeJonge PM, Callear AP, Bazzi LA, Capriola SB, Malosh RE, et al. Coronavirus
777 Occurrence and Transmission Over 8 Years in the HIVE Cohort of Households in Michigan. *The*
778 *Journal of Infectious Diseases.* 2020 Jun 16;222(1):9–16.
- 779 48. KSH. H-UNCOVER – Reprezentatív felmérés a koronavírus elleni küzdelemben – eredmények
780 [Internet]. KSH; Available from:
781 http://www.ksh.hu/huncover_reprezentativ_felmeres_eredmenyek
- 782 49. Official COVID19 Dashboard public information [Internet]. Federal Ministry Republic of
783 Austria, Social Affairs, Health, Care and Consumer Protection; 2020. Available from:
784 <https://info.gesundheitsministerium.at/?l=en>
- 785 50. COVID-19: epidemiological update of March 4, 2020. [Internet]. Public Health France; 2020
786 Mar. Available from: [https://www.santepubliquefrance.fr/dossiers/coronavirus-covid-](https://www.santepubliquefrance.fr/dossiers/coronavirus-covid-19/coronavirus-chiffres-cles-et-evolution-de-la-covid-19-en-france-et-dans-le-monde#block-266156)
787 [19/coronavirus-chiffres-cles-et-evolution-de-la-covid-19-en-france-et-dans-le-monde#block-](https://www.santepubliquefrance.fr/dossiers/coronavirus-covid-19/coronavirus-chiffres-cles-et-evolution-de-la-covid-19-en-france-et-dans-le-monde#block-266156)
788 [266156](https://www.santepubliquefrance.fr/dossiers/coronavirus-covid-19/coronavirus-chiffres-cles-et-evolution-de-la-covid-19-en-france-et-dans-le-monde#block-266156)

- 789 51. Coronavirus Disease 2019 (COVID-19) Daily Situation Report of the Robert Koch Institutue.
790 [Internet]. Robert Koch Institutue; 2020 Mar. Available from:
791 [https://www.rki.de/DE/Content/InfAZ/N/Neuartiges_Coronavirus/Situationsberichte/2020-03-](https://www.rki.de/DE/Content/InfAZ/N/Neuartiges_Coronavirus/Situationsberichte/2020-03-04-en.pdf?__blob=publicationFile)
792 [04-en.pdf?__blob=publicationFile](https://www.rki.de/DE/Content/InfAZ/N/Neuartiges_Coronavirus/Situationsberichte/2020-03-04-en.pdf?__blob=publicationFile)
- 793 52. Rosini. Cases tested people tested / tested cases [github] [Internet]. github; Available from:
794 [https://github.com/pcm-dpc/COVID-19/blob/master/dati-regioni/dpc-covid19-ita-regioni-](https://github.com/pcm-dpc/COVID-19/blob/master/dati-regioni/dpc-covid19-ita-regioni-20200304.csv)
795 [20200304.csv](https://github.com/pcm-dpc/COVID-19/blob/master/dati-regioni/dpc-covid19-ita-regioni-20200304.csv)
- 796 53. Report on confirmed COVID-19 cases in Spain. [Internet]. Carlos III. Health Institute; 2020 Mar.
797 Available from: <https://cnecovid.isciii.es/covid19/#ccaa>
- 798 54. Iran COVID-19 death now 77 as emergency services chief infected. Channel New Asia
799 [Internet]. 2020 Mar 4; Available from: [https://www.channelnewsasia.com/news/world/covid19-](https://www.channelnewsasia.com/news/world/covid19-coronavirus-death-toll-iran-77-mar-3-12496192)
800 [coronavirus-death-toll-iran- 77-mar-3-12496192](https://www.channelnewsasia.com/news/world/covid19-coronavirus-death-toll-iran-77-mar-3-12496192)
- 801 55. Reustle S. Japan COVID-19 Coronavirus Tracker. [Internet]. Available from:
802 <https://covid19japan.com>
- 803 56. MOH, Singapore. ONE MORE CASE DISCHARGED; TWO NEW CASES OF COVID-19
804 INFECTION CONFIRMED [Internet]. Singapore: Ministry of Health; 2020 Mar. Available
805 from: [https://www.moh.gov.sg/news-highlights/details/one-more-case-discharged-two-new-](https://www.moh.gov.sg/news-highlights/details/one-more-case-discharged-two-new-cases-of-covid-19-infection-confirmed)
806 [cases-of-covid-19-infection-confirmed](https://www.moh.gov.sg/news-highlights/details/one-more-case-discharged-two-new-cases-of-covid-19-infection-confirmed)
- 807 57. No. of COVID-19 Cases in S. Korea Rises to 5,621 [Internet]. KBS World Radio; 2020 Mar.
808 Available from: http://world.kbs.co.kr/service/news_view.htm?lang=e&Seq_Code=151776
- 809 58. Pastor-Satorras R, Vespignani A. Epidemic Spreading in Scale-Free Networks. *Phys Rev Lett.*
810 2001 Apr 2;86(14):3200–3.
- 811 59. Meyers LA, Pourbohloul B, Newman MEJ, Skowronski DM, Brunham RC. Network theory and
812 SARS: predicting outbreak diversity. *Journal of Theoretical Biology.* 2005 Jan;232(1):71–81.
- 813 60. Sapiezynski P, Stopczynski A, Lassen DD, Lehmann S. Interaction data from the Copenhagen
814 Networks Study. *Sci Data.* 2019 Dec;6(1):315.
- 815 61. WHO. Considerations for quarantine of contacts of COVID-19 cases [Internet]. 2020 Aug.
816 Available from: [https://www.who.int/publications/i/item/considerations-for-quarantine-of-](https://www.who.int/publications/i/item/considerations-for-quarantine-of-individuals-in-the-context-of-containment-for-coronavirus-disease-(covid-19))
817 [individuals-in-the-context-of-containment-for-coronavirus-disease-\(covid-19\)](https://www.who.int/publications/i/item/considerations-for-quarantine-of-individuals-in-the-context-of-containment-for-coronavirus-disease-(covid-19))
- 818 62. Stopczynski A, Pentland A ‘Sandy’, Lehmann S. How Physical Proximity Shapes Complex
819 Social Networks. *Sci Rep.* 2018 Dec;8(1):17722.
- 820 63. Berthold MR, Cebon N, Dill F, Gabriel TR, Kötter T, Meinel T, et al. KNIME: The Konstanz
821 Information Miner. In: Preisach C, Burkhardt H, Schmidt-Thieme L, Decker R, editors. *Data*
822 *Analysis, Machine Learning and Applications.* Berlin, Heidelberg: Springer Berlin Heidelberg;
823 2008. p. 319–26.
- 824 64. Csárdi G, Nepusz T. Igraph - The network analysis package [Internet]. 2006. Available from:
825 <https://igraph.org>

- 826 65. Albert R, Jeong H, Barabási A-L. Error and attack tolerance of complex networks. *Nature*. 2000
827 Jul 27;406(6794):378–82.
- 828 66. Feld SL. Why Your Friends Have More Friends Than You Do. *American Journal of Sociology*.
829 1991 May;96(6):1464–77.
- 830 67. Cohen R, Havlin S, ben-Avraham D. Efficient Immunization Strategies for Computer Networks
831 and Populations. *Phys Rev Lett*. 2003 Dec 9;91(24):247901.
- 832 68. Knime workflow [Internet]. Available from:
833 <https://univet.hu/en/research/dfi/publications/scientific-publications/covid-19/>
- 834 69. Adamecz-Völgyi A, Szabó-Morvai Á. Kik dolgoznak a frontvonalban? [Internet]. MTA
835 Közgazdaság- és Regionális Tudományi Kutatóközpontja; 2020 Apr. Available from:
836 <https://www.mtakti.hu/koronavirus/kik-dolgoznak-a-frontvonalban/13090/>
- 837 70. Miller A, Reandelar MJ, Fasciglione K, Roumenova V, Li Y, Otazu GH. Correlation between
838 universal BCG vaccination policy and reduced mortality for COVID-19. *medRxiv*. 2020 Sep 14;
- 839 71. Berg MK, Yu Q, Salvador CE, Melani I, Kitayama S. Mandated Bacillus Calmette-Guérin
840 (BCG) vaccination predicts flattened curves for the spread of COVID-19 [Internet]. *Public and*
841 *Global Health*; 2020 Apr [cited 2020 Nov 25]. Available from:
842 <http://medrxiv.org/lookup/doi/10.1101/2020.04.05.20054163>
- 843 72. HUNgarian COronaVirus Disease-19 Epidemiological Research [Internet]. Semmelweis
844 University Heart and Vascular Center; 2020 Jun. Available from:
845 <https://clinicaltrials.gov/ct2/show/study/NCT04370067>
- 846 73. Oliver N, Lepri B, Sterly H, Lambiotte R, Deletaille S, De Nadai M, et al. Mobile phone data for
847 informing public health actions across the COVID-19 pandemic life cycle. *Sci Adv*. 2020
848 Jun;6(23):eabc0764.
- 849

850 **1 Figure captions**

851 Figure 1.

852 Structure of the modified SEIR model with compartment initials (Susceptible, Exposed (Latent),
853 Infected, Recovered), transitions from one compartment to another (full line), parameters and routes
854 of infection (dashed line). Susceptible individuals can get the infection either from individuals being
855 in the Infected compartment with the rate of β , or from Exposed compartment (latent individuals)
856 with the rate of β_L .

857 Figure 2.

858 Distribution of Infected individuals in *Scenarios 1 to 3*.

859 Figure 3.

860 Distribution of Exposed (latent) individuals in *Scenarios 1 to 3*.

861 Figure 4.

862 Comparison of the distribution of Infected individuals in case of modified SEIR model and basic
863 SEIR model in case of *Scenario 1*.

864 Figure 5.

865 Results of sensitivity analysis of the modified SEIR model: changes in daily maximum value of
866 individuals in the infected compartment (A) and changes in the number of the days related to the
867 former endpoint (B)

868 Figure 6.

869 Epidemic thresholds (λ'_c) of different degree exponents (γ) and target degrees (k_t) calculated to
870 increase the epidemic threshold above the spreading rate of COVID-19 with targeted sampling. The
871 spreading rate (λ) of the virus is set to 0.067 (red line).

872

Figures

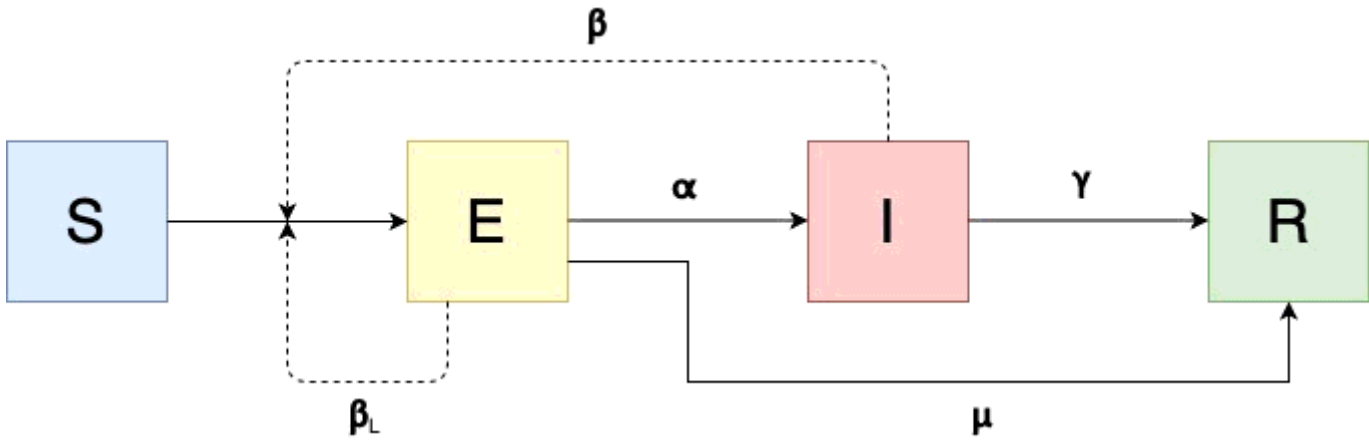


Figure 1

Structure of the modified SEIR model with compartment initials (Susceptible, Exposed (Latent), Infected, Recovered), transitions from one compartment to another (full line), parameters and routes of infection (dashed line). Susceptible individuals can get the infection either from individuals being in the Infected compartment with the rate of β , or from Exposed compartment (latent individuals) with the rate of β_L .

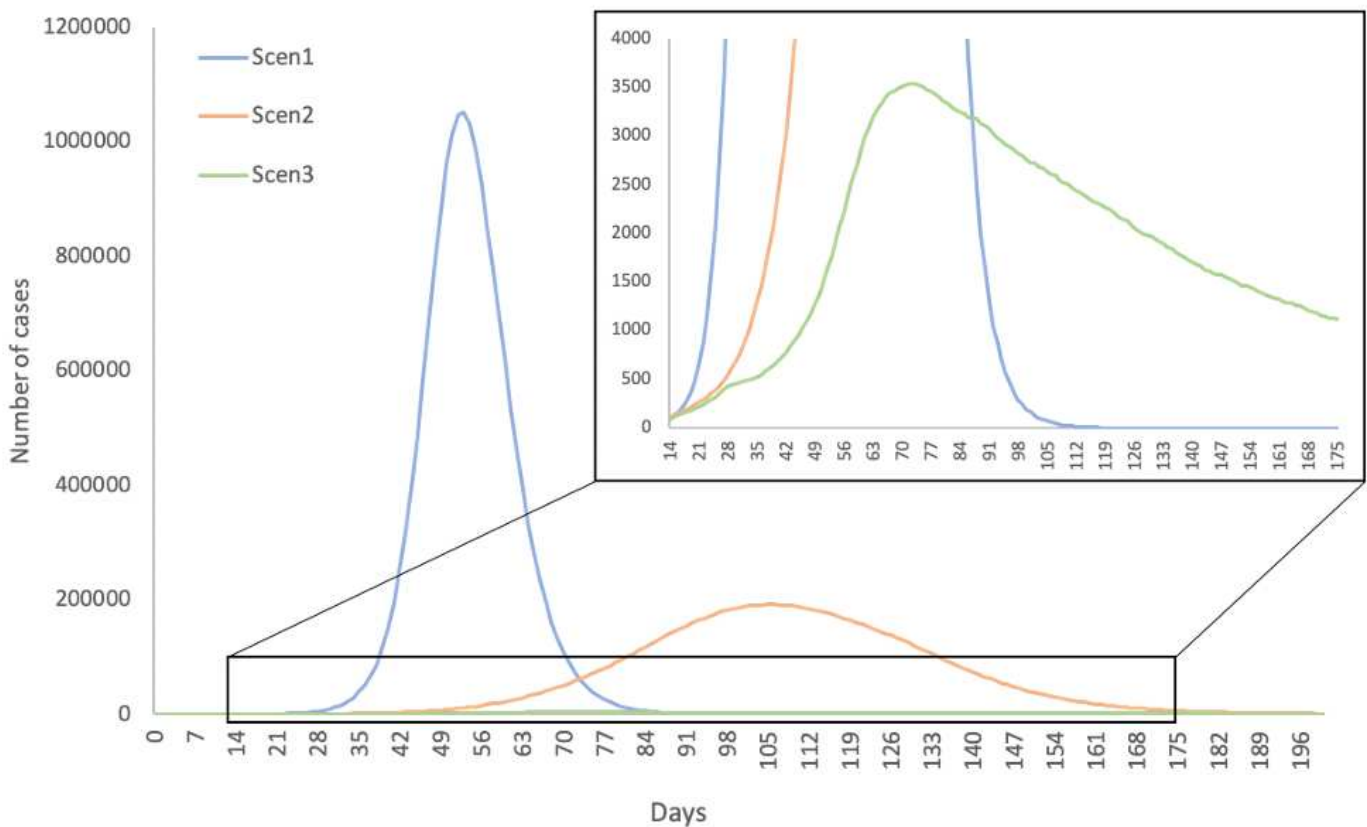


Figure 2

Distribution of Infected individuals in Scenarios 1 to 3

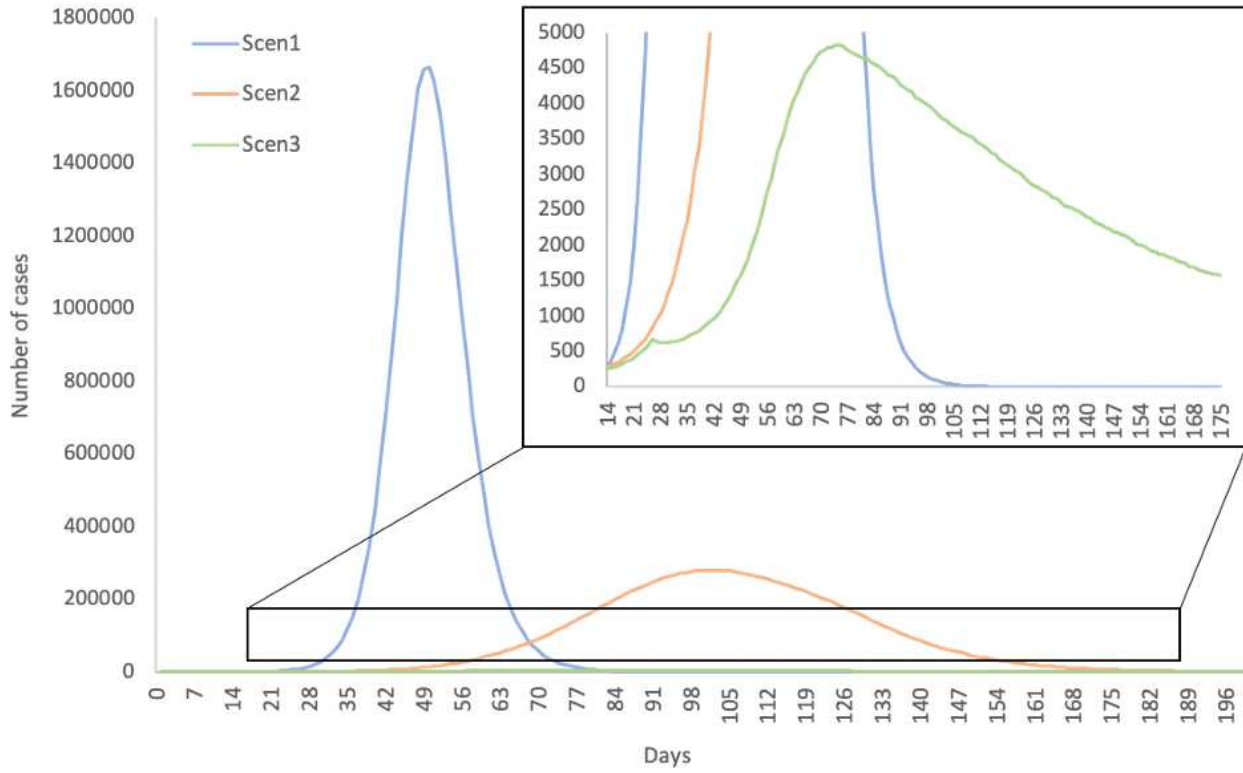


Figure 3

Distribution of Exposed (latent) individuals in Scenarios 1 to 3.

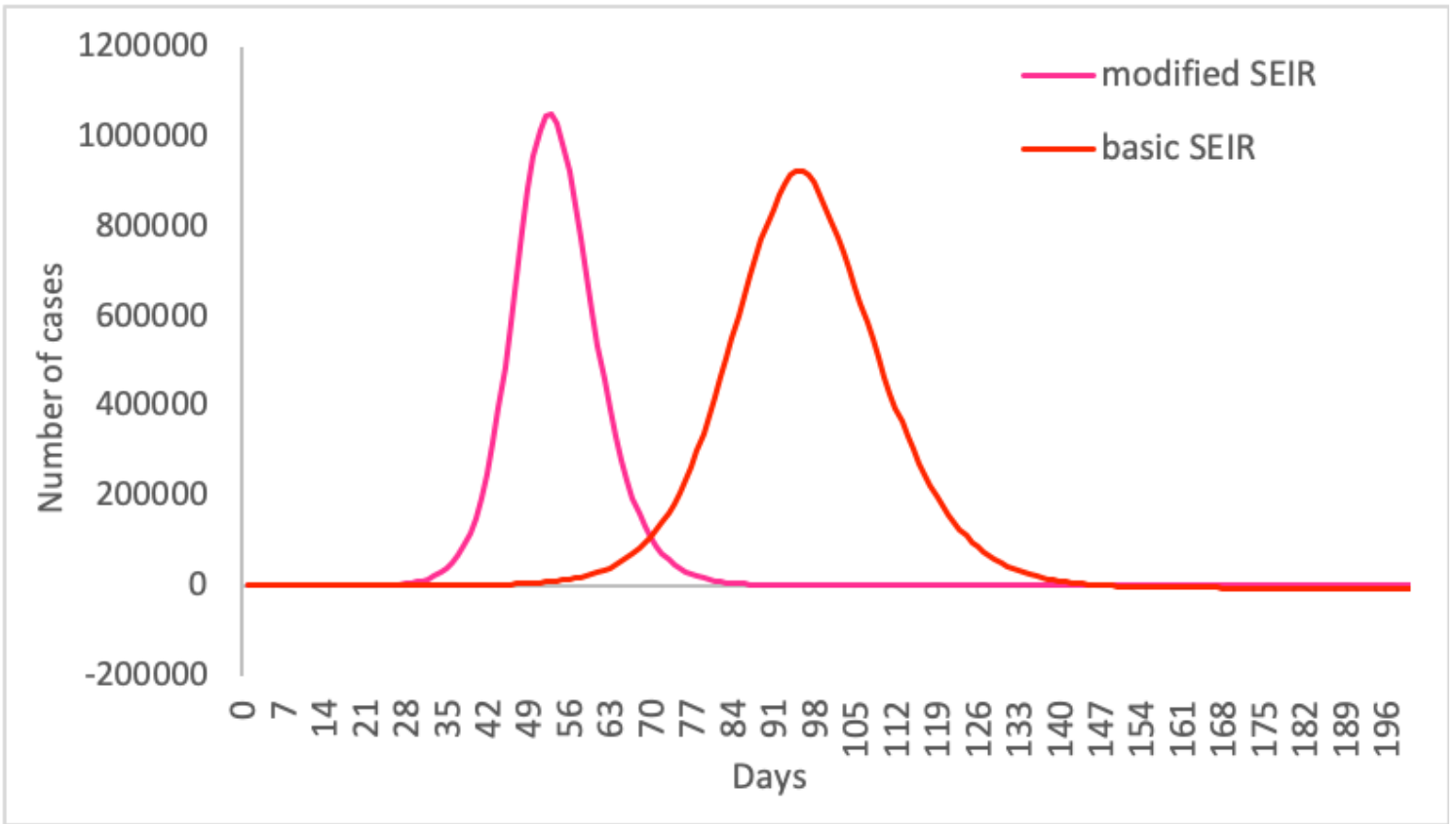


Figure 4

Comparison of the distribution of Infected individuals in case of modified SEIR model and basic SEIR model in case of Scenario 1

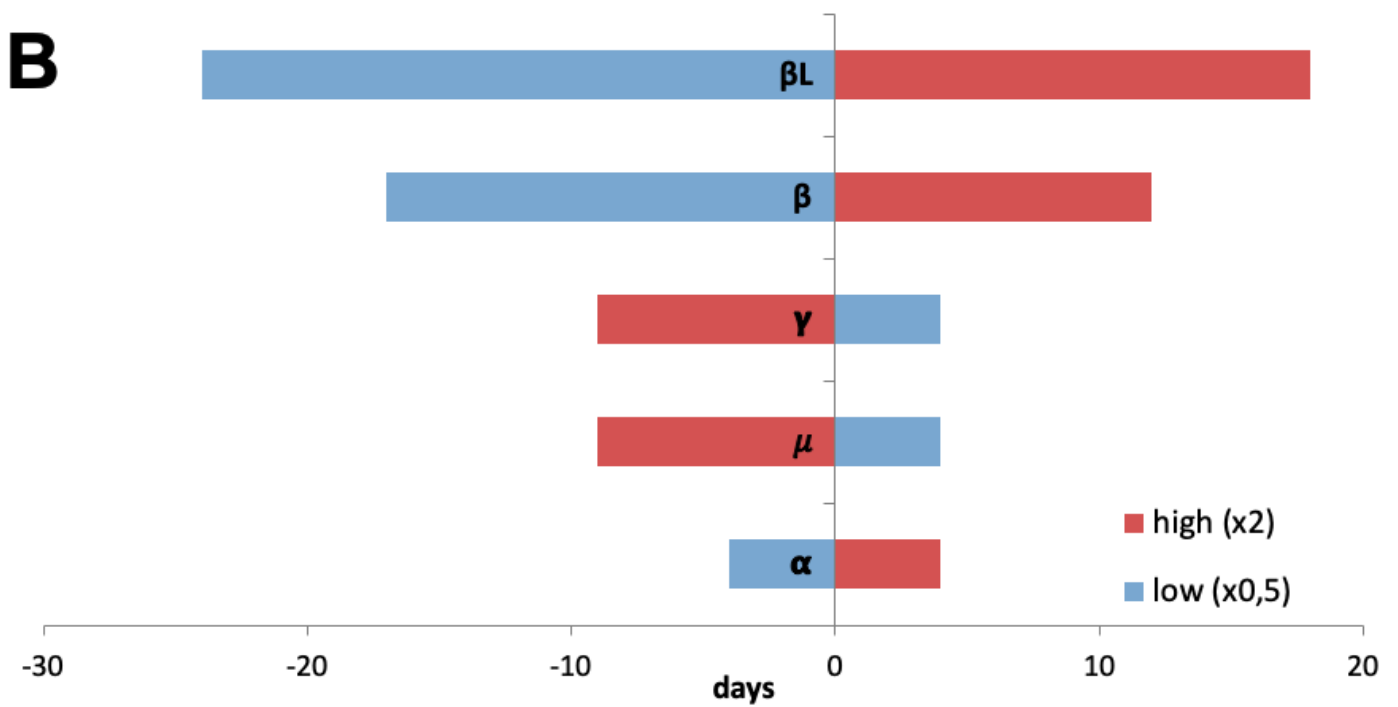
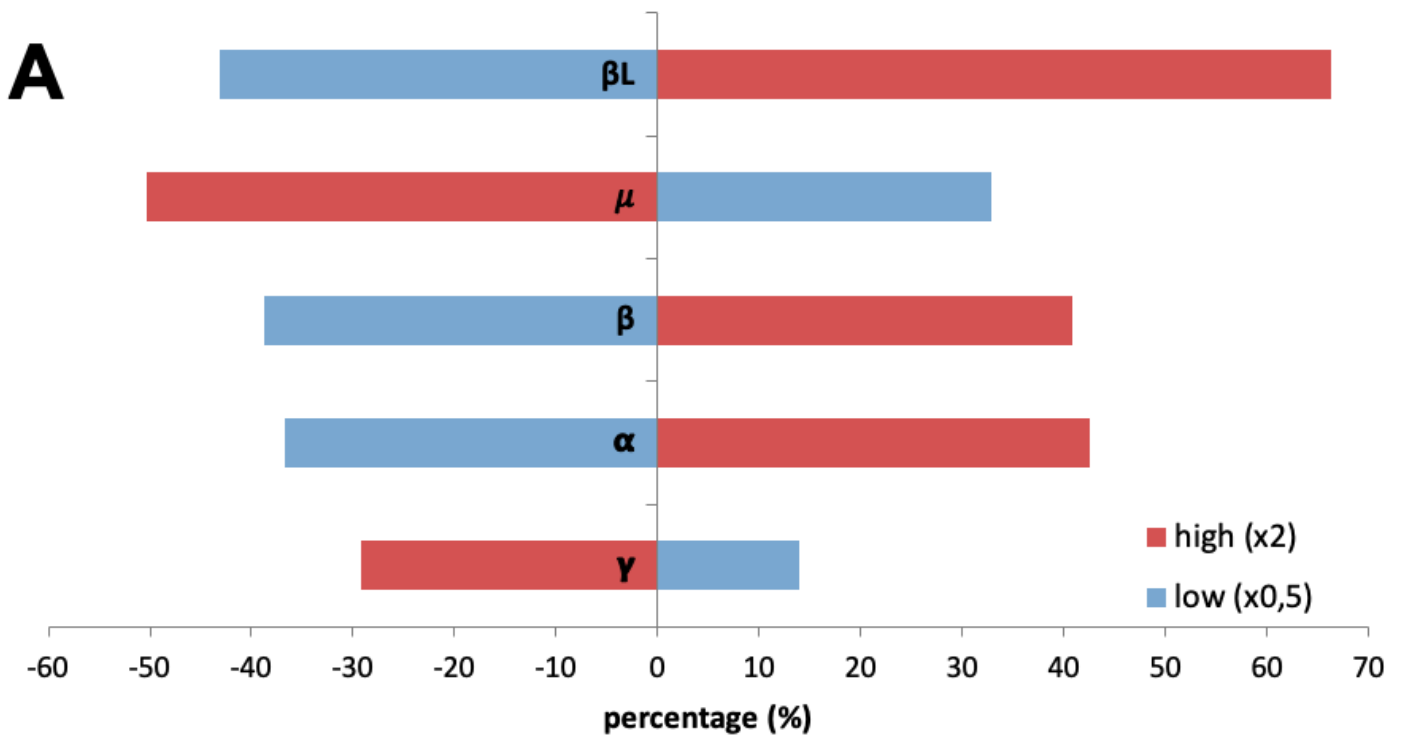


Figure 5

Results of sensitivity analysis of the modified SEIR model: changes in daily maximum value of individuals in the infected compartment (A) and changes in the number of the days related to the former endpoint (B)

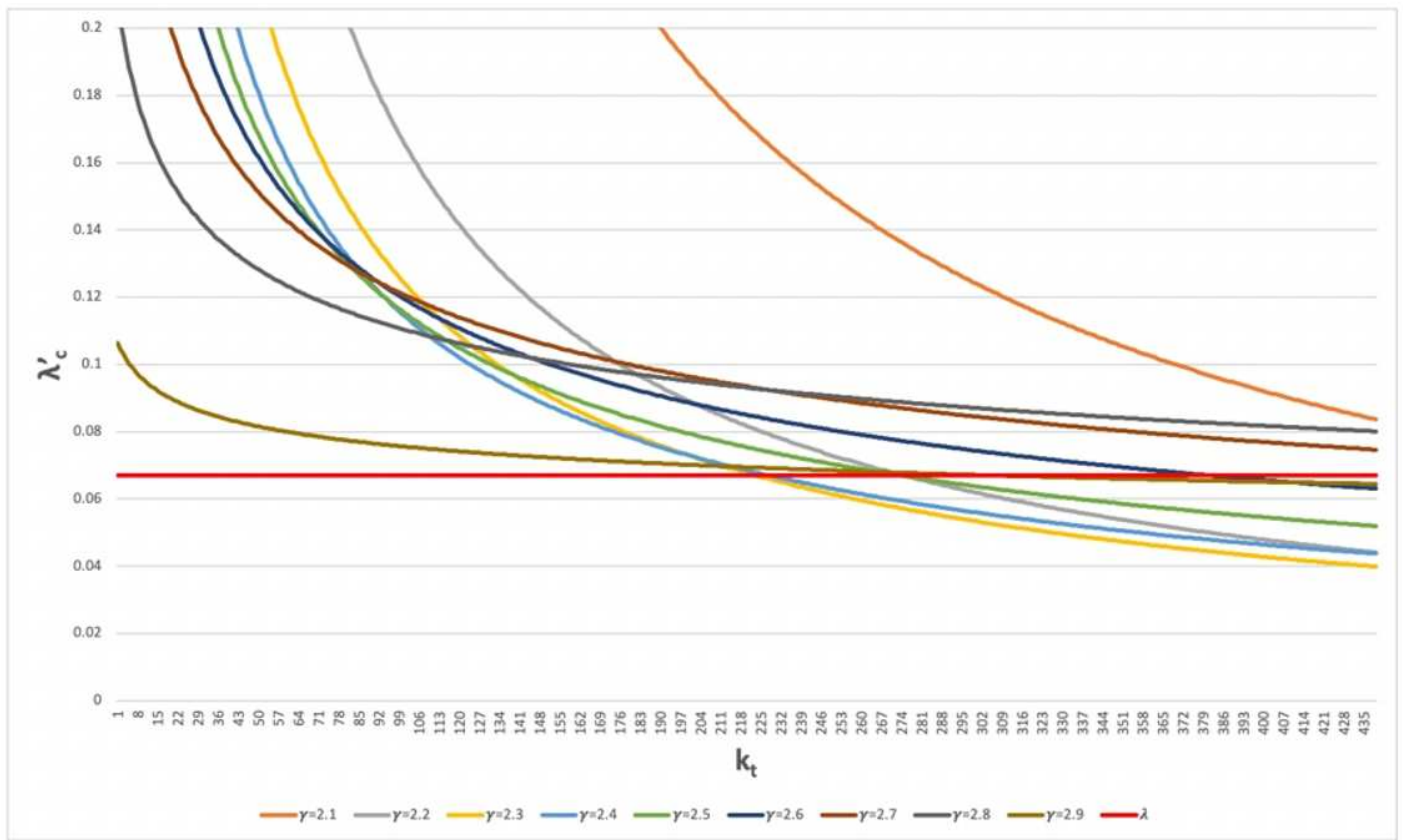


Figure 6

Epidemic thresholds (λ'_c) of different degree exponents (γ) and target degrees (k_t) calculated to increase the epidemic threshold above the spreading rate of COVID-19 with targeted sampling. The spreading rate (λ) of the virus is set to 0.067 (red line).